co2amp

Mikhail Polyanskiy

September 5, 2014

Contents

Chapter 1

General notes

1.1 Program capabilities

1. Ultrashort pulse amplification in CO_2 active medium
   - Rotational numbers up to J=60
   - Hot- and sequence- bands
   - Isotopic CO_2
2. Molecular dynamics
   - Realistic pumping
   - Collisional relaxation processes
   - Stimulated transitions
   - Independent consideration of active media regions at different elongation from optical axis
3. Diffraction-based beam propagation
   - Beam manipulation with common optical elements
   - Arbitrary optical configuration
4. Linear dispersion and non-linear effects in optical materials
   - Pulse chirping
   - Kerr lensing
   - Self-phase modulation
5. Advanced optics
   - Chirped-pulse amplification
   - Trains of pulses
   - Staging (program output as an input for the next stage stage)
6. User's interface
   - Easy parameter specification
   - Graphical output
   - Save/recall your work

1.2 Availability

The entire code base of the `co2amp` program is published in the GitHub website (`https://github.com/polyanskiy/co2amp`) and is freely available for use, modification and re-distribution under the terms of the General Public License (GPL) (`http://www.gnu.org/copyleft/gpl.html`). The binary package is provided in the form of a Windows installer that contains pre-compiled executables, documentation and the source-code (all found in the installation directory after installation) at `https://github.com/polyanskiy/co2amp/releases`. User interface is built using a cross-platform library QT (`http://qt-project.org/`) and thus should compile under other platforms supported by QT (MacOS, Linux). Third-party components used in the package (`gnuplot`, `7-zip`) are also freely available for multiple platforms (`http://www.gnuplot.info/`, `http://www.7-zip.org/`).

1.3 Acknowledgements

Viktor Platonenko provided the Mathcad code for pulse amplification in the CO_2 active medium that was used as a starting point of the development of the `co2amp` code; he also provided valuable input on the early stage of the work.

Chapter 2

Getting started manual

2.1 Basic concepts

The `co2amp` code allows simulating propagation of an ultrashort pulse through an arbitrary optical system that can include CO_2 amplifiers. Pulse amplification and fast molecular dynamics (stimulated transitions, rotational relaxation) calculations are performed in time domain in the time-frame moving with the pulse. Processes that are much slower than the pulse duration (discharge pumping, vibrational relaxation) are modelled separately in the laboratory time-frame. The program input parameters include initial pulse characteristics, optical configuration, active medium composition and excitation parameters (e.g. discharge profile), and number of nodes in the calculation grids for the time- (pulse time frame) and space- (radial) coordinates. Axial symmetry is assumed at all times. Optical system can include multiple amplifiers if they have same gas composition and pumping dynamics; sequential amplification in different amplifiers can be modeled using the staging option as described later. Temporal pulse shape (averaged across the beam) and beam profile (averaged for the entire pulse duration) at every element of the optical layout are saved and can be accessed in both graphical and tabulated-numerical representation. Complete pulse/beam information (complex field in every node of the time-space calculation grid) at the output of the system can also be saved and used as an input for another system (staging). The user interface program allows saving all inputs and outputs of the calculations as a single compressed file ('.co2' or '.co2x' extension). The difference between the two formats is that the files with extension ending with 'x' ("extended") include the complete output field record and thus are suitable for staged calculations. Fig. 2.1 shows the user interface of the `co2amp` program described in the following sections.

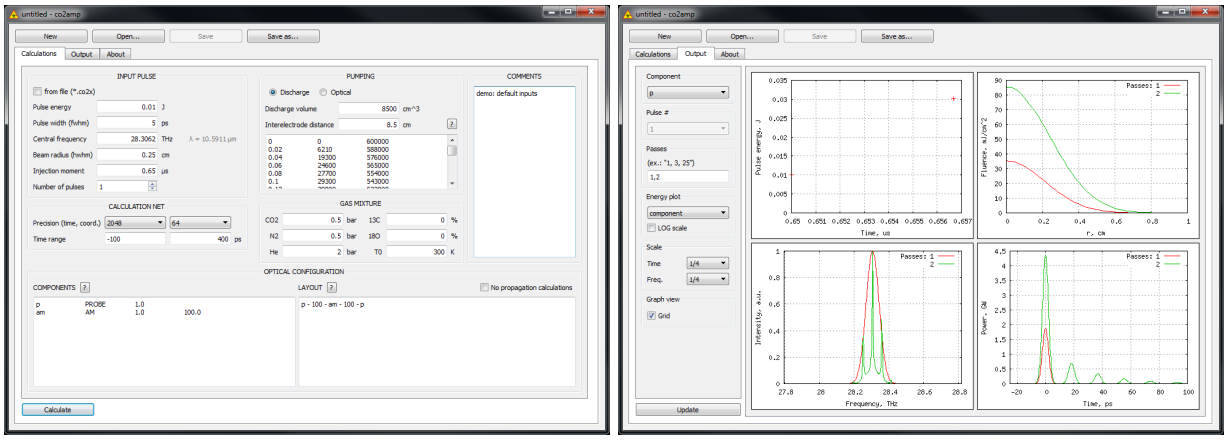

Figure 2.1: `co2amp` user interface: Input- (left) and output- (right) tabs.

2.2 Input pulse and calculation grid

Unless the output of another simulation is used as an input (staged calculations), both temporal shape of the input pulse and the input beam profile are assumed to be Gaussian; and the pulse is assumed to be transform-limited (no initial chirping). Pulse energy, duration, central frequency, and beam radius are entered in the corresponding fields in the input tab. "Injection moment" parameter specifies the time-delay between the beginning of the pumping of the active medium and pulse injection into the optical system. It is also possible to simulate amplification of a train of identical and equidistant pulses; number of pulses in the train and time-delay between them must be specified in this case. Number of nodes in the calculation grid has to be specified for the radial coordinate and for the fast time-frame associated with the pulse (time-frame for the slow processes uses a fixed 1-ns step and does not require a user input). Number of nodes is always a power of two that allows utilization of fast Fourier transform (FFT) algorithms. Calculations with a larger number of nodes are usually more accurate but, on the other hand, take longer and require more computer memory (both calculation time and required memory are roughly proportional to the product of the number of nodes in the time- and space- grids). This is therefore recommended to start from running the simulation with a smaller number of nodes and then repeat it several times, each time with a denser grid. Absence of considerable change in the program output with increase of the number of nodes will indicate that the grid density is sufficient. Limits of the pulse time-frame ("time range") specify the time interval considered in the calculations. Initially, the pulse is centered at $t = 0$ and it tends to shift to the longer delays upon amplification due to the limited medium response time and spectrum modulation. Thus, optimum time range is usually asymmetric with a short negative and a longer positive part. Time-step $\Delta t = (t_{max} - t_{min})/(n_0 - 1)$, where t_{max} and t_{min} define the time range and n_0 is the number of nodes in the time grid, must be small enough to accurately describe the pulse profile at all stages of the propagation through the optical system. It is also important to keep in mind that time range and number of nodes in the time grid also define the range and step in the frequency domain: $\Delta\nu = 1/(t_{max} - t_{min})$ and $(\nu_{max} - \nu_{min}) = 1/\Delta t$. This means that the time range must be long enough to provide sufficient resolution in the frequency domain and at the same time the time step must be sufficiently short to provide a bandwidth that fits the whole spectral region of interest. Maximum radial coordinate is defined separately for every element of the optical system. This is described in the next section. Identifying an appropriate calculation grid is very important for building an accurate model of an optical system. An effort put in this part of the simulation process will pay off by fast and reliable calculations.

2.3 Optical layout and beam propagation

The `co2amp` code uses a concept of optical surfaces similar to that employed in the ray-tracing algorithms. In this concept optical system is represented by a series of thin optical components (surfaces) each of which can alter the wave front. Between surfaces, beam propagates undisturbed. In order to specify the optical system one has to 1) describe all optical components and 2) describe the location of the components in respect to each other. In `co2amp`'s user interface program, this is done by editing text in the two dedicated fields ("Components" and "Layout"). The format of these fields is described below.

2.3.1 Components

Each optical component is described in a separate line by several tab- or space- separated entries:

- Entry 1 '***ID***': An arbitrary user-defined alpha-numeric string for identifying the component;
- Entry 2 '***Type***': Type of the component; must be one of the types listed in the table;
- Entry 3 '***Field***': Maximum radial coordinate in centimeters to be considered in the simulations;
- Entry 4 '***Parameter 1***' and Entry 5 '***Parameter 2***': Meaning of these fields depend on the type of the component as summarized in the table:

Type	Description	***Parameter 1***	***Parameter 2***
`AM`	Active medium	Length [cm]	-
`PROBE`	Passive surface, may be used as limiting aperture	-	-
`MASK`	Opaque circular screen	Radius [cm]	-
`ABSORBER`	Absorber	Transmittance	-
`LENS`	Ideal lens (no spherical or chromatic aberrations)	Focal length [cm]	-
`WINDOW`	Transparent flat window (zero reflection- and absorption- losses)	Window material: KCl, NaCl, ZnSe, GaAs, CdTe, Ge, or Si	Thickness [cm]
`STRETCHER`	Stretcher or compressor	Pulse chirping [ps/THz] (positive for red-chirp)	-

The following example defines several 2.5-cm diameter components: A probe surface, two 120-cm-long amplifier sections, a 5-cm-thick NaCl window and an absorber for modelling 4% reflection losses:

```
p     PROBE      1.25
am1   AM         1.25   120
am2   AM         1.25   120
win   WINDOW     1.25   NaCl   5
abs   ABSORBER   1.25   0.96
```

2.3.2 Layout

Optical configuration is specified as a sequence of the components identified by their ***ID***'s. All components are separated by non-negative distances expressed in centimeters. Components and distances must be separated by spaces, tabs, new-line symbols or dashes. The following is an example of an optical configuration that uses the components defined in the previews example:

```
p-0-abs-0-win-0-abs-100-am1-200-am2-100-abs-0-win-0-abs-0-p
```

This example defines the configuration shown in the Fig. 2.2.

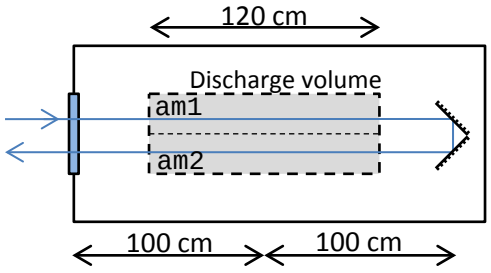

Figure 2.2: Example optical configuration.

In this example beam propagates twice through the same amplifier. However, we consider this configuration as two identical but independent active volumes (`am1` and `am2`) because at each pass the beam interacts with a different zone of the active medium.

2.3.3 Beam propagation

When two components of an optical configuration are separated by a non-zero distance, beam propagation between them is simulated using the Huygens-Fresnel diffraction integral in the assumption of axial symmetry. Propagation is simulated separately for each moment of time from the time calculation grid. Optical surface model assumes that components of the optical layout are infinitely thin. Propagation is calculated between the middle points of the components; for the purpose of simulating pulse interaction with a prolonged optical element, beam is assumed to be collimated inside this element. For instance, the sequence of calculations for the previews example is:

1. Interaction with the window (including reflection losses);
2. 100 cm propagation to the middle of the first pass through the amplifier (no amplification so far);
3. Amplification by a 120-cm amplifier section assuming that the beam is collimated;
4. 200 cm (100×2) propagation to the middle of the second pass through the active volume;
5. Amplification by the second 120-cm amplifier section assuming that the beam is collimated;
6. 100 cm propagation to the window;
7. Interaction with the windows.

Accuracy of the model can be improved if one divides a long amplifier into several shorter sub-sections. For instance, we can modify our example configuration as shown in the Fig. 2.3.

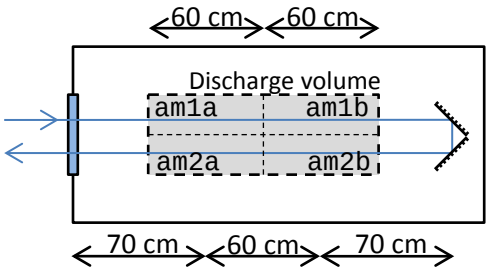

Figure 2.3: Example configuration modified for improved accuracy.

Components and Layout entries for the modified configuration are as follows:

Components:

```
p      PROBE      1.25
am1a   AM         1.25   60
am1b   AM         1.25   60
am2a   AM         1.25   60
am2b   AM         1.25   60
win    WINDOW     1.25   NaCl   5
abs    ABSORBER   1.25   0.96
```

Layout:

```
p-0-abs-0-win-0-abs-70-am1a-60-am1b-140-am2b-60-am2a-70-abs-0-win-0-abs-0-p
```

Population dynamics in all amplifier sections is modeled separately and thus splitting a long amplifier into shorter sections provides also a more realistic model of the active medium.

2.4 Active medium and amplification

All active medium sections used in a single simulation must have same gas composition and pumping conditions (staged simulations can be used for complex systems with two or more non-identical amplifiers). Composition (including isotopic enrichment of carbon dioxide) and initial temperature of the active medium are specified in the "Gas Mixture" fields of the input tab of the user interface. Pumping by electric discharge is the primary pumping scheme of the `co2amp` code. Rudimentary support for optical pumping is also included but not discussed here. For discharge pumping, geometry of the discharge volume (discharge volume and the distance between electrodes) and discharge profile (tabulated values of discharge current expressed in amperes and voltage in volts at time moments in microseconds) must be provided. Pumping dynamics calculations are done using a Boltzmann equation that takes into account elastic collisions between electrons and molecules and inelastic collisions with molecular rotational-, vibrational- and electronic- excitations and ionization. Tabulated empirical values of corresponding cross-sections as functions of electron energy are used. The Boltzmann equation is solved repeatedly in order to accurately describe the variation of pumping efficiency by the electric field varying during the discharge.

2.5 Program output

The output of the program is given as a temporal pulse structure and its spectrum (both averaged across the beam) and beam profile (averaged on the duration of the pulse) at each element of the optical layout. The user can chose an optical component to display from the list of all the available components. In the case if the selected component is used several times in the optical configuration, it is also possible to specify which passes through the component will be displayed. Also, integral pulse energy can be provided either at every pass through a selected component or at all passes through all components of the system layout. Output for the layout components of type `AM` (active medium) provides additional information that includes gain, discharge profile, population dynamics, and the dynamics of pumping energy distribution (fractions of discharge energy going into excitation of laser levels and excitation of molecular translations and ionization). Right-mouse-click on a figure allows the user to copy either the graphics or the numerical data for future use.

Chapter 3

Models

3.1 Molecular dynamics

Simulations of active medium pumping by electric discharge and vibrational relaxation are done following Karlov and Konev [1].

3.1.1 Pumping by electric discharge

Pumping is described by the Boltzmann equation in the following form (Karlov and Konev cite [2] and [3])

$$
\begin{aligned}
-\frac{1}{3}\left(\frac{E}{N}\right)^2 \frac{d}{du}\left[u\left(\sum_j y_j Q_{mj}(u)\right)^{-1}\frac{df}{du}\right] \quad = \\
1.09\times 10^{-3}\frac{d}{du}\left[u^2 f\sum_j \frac{y_j}{M_j}Q_{mj}(u)\right] \quad + \quad \sum_{j=1,2} y_j C_j \frac{d}{du}(uf) \quad + \quad 6By_2\frac{d}{du}\left(uQ(u)f\right) \\
+ \quad \sum_j y_j \sum_k (u+u_{jk})Q_{jk}(u+u_{jk})f(u+u_{jk}) \quad - \quad (uf)\sum_j y_j \sum_k Q_{jk}(u)
\end{aligned}
\tag{3.1}
$$

where left part describes energy of electrons in the electric field, the first component of the sum of the right part represents energy transfer via elastic collisions between electrons and molecules, second and third components describe collisions with molecular rotation excitation, and the two last components relate to inelastic collisions with transfer of the energy u_{jk} into vibrational and electronic excitation and ionization.

Electron energy u is expressed in eV;

Ration of the field to the full molecular density E/N is expressed in the units of 10^{-16} V·cm^2;

y_j are the relative molecule concentrations ($j = 1$ corresponds to CO_2, $j = 2$ to N_2 and $j = 3$ to He);

$M_1 = 44$, $M_2 = 28$, $M_3 = 4$ are the molar masses,

$C_1 = 8.2\times 10^{-4}$ eV·Å^2 [4];

$C_2 = 5.06\times 10^{-4}$ eV·Å^2 [5];

$B = 2.5\times 10^{-4}$ is the N_2 rotational constant;

Effective crossections are expressed in Å; their numerical values in the nodes are given in the tables below (linear interpolation must be used for determining the values in intermediate points); the data and citations are reproduced from [1].

The following notation for cross-sections is used:

Q_{m1} - Transport cross-section of CO_2 [6];

Q_{m2} - Transport cross-section of N_2 [5];

Table 3.1: Tabulated data on the cross-sections for discharge pumping

u_i	Q_{m1}	u_i	Q_{m2}	u_i	Q_{m3}	u_i	Q
0	140	0	1.4	0	5	0.0015	0
0.04	84	0.001	1.4	0.01	5.4	0.05	0.1
0.1	55	0.002	1.6	0.1	5.8	0.25	0.65
0.3	21	0.008	2	0.2	6.2	0.5	1.15
0.5	10.8	0.01	2.2	1	6.5	0.8	2
0.6	9.4	0.04	4	2	6.1	1	2.65
1	5.7	0.08	6	7	5	1.5	5.6
1.7	5	0.1	6.5	10	4.1	1.8	7.5
2	5.1	0.2	8.8	20	3	1.9	8.2
2.5	6	0.3	9.8			2	8.6
3	7.7	0.4	10			2.15	8.95
4.1	9.4	1	10			2.43	9
5	14.5	1.2	11			2.6	8.9
7.4	10	1.4	12.5			2.75	8.4
10	11.7	1.8	20			2.9	7.65
20	16	2	25			3.25	6.2
27	16.3	2.5	30			3.6	5.1
50	13	3	26			4	4.5
		4	15			4.5	4.16
		5	12			5	3.97
		7	10			5.5	3.93
		10	10			7	4.17
		14	11			9	4.46
		18	12.2			11	4.42
		20	12			15	3.94
		30	10			22	3.15
		100	10			25	3.05

Table 3.2: Tabulated data on the cross-sections for discharge pumping - continued 1

u_i	Q_{11}	u_i	Q_{12}	u_i	Q_{13}	u_i	Q_{14}	u_i	Q_{15}
0.083	0	0.167	0	0.252	0	2.37	0	2.37	0
0.085	0.36	0.2	0.54	2.7	0.25	3	0.26	3	0.17
0.09	1.04	0.25	0.82	3	0.4	3.5	0.52	3.65	0.33
0.1	1.6	0.3	0.82	3.3	0.6	4	0.5	3.8	0.31
0.12	1.84	0.5	0.68	3.6	0.65	4.5	0.22	4	0.21
0.14	2.12	0.7	0.56	4.5	0.23	4.6	0.1	4.3	0.1
0.16	2.16	1	0.47	4.6	0.1	5	0	5	0
0.2	2.08	1.4	0.45	5	0				
0.3	1.76	2	0.55						
0.4	1.52	3	1.15						
0.5	1.28	3.9	1.83						
0.6	1.08	4.5	1.4						
0.8	0.8	5	0.4						
1	0.58	6	0.28						
1.2	0.48	10	0.2						
1.6	0.34	20	0.1						
1.8	0.35								
2	0.4								
2.5	0.64								
3	1.04								
3.7	1.4								
4	1.36								
4.2	1.2								
4.5	0.92								
5	0.53								
6	0.4								
8	0.36								
9	0.28								
10	0.16								
10.1	0								
$u_{11} = 0.083$ eV		$u_{12} = 0.167$ eV		$u_{13} = 0.252$ eV		$u_{14} = 0.339$ eV		$u_{15} = 0.422$ eV	

u_i	Q_{16}	u_i	Q_{17}	u_i	Q_{18}	u_i	Q_{19}	u_i	$Q_{1,10}$
2.5	0	0.29	0	7	0	10.5	0	13.8	0
3	0.19	0.3	0.44	8	0.5	11.5	0.56	15	0.1
3.6	0.245	0.35	0.65	8.4	0.6	14	0.8	16	0.13
4	0.21	0.4	0.73	9	0.46	20	1.2	17	0.17
5.07	0	0.5	0.84	10	0.175	30	2	30	1.55
		0.8	1	10.5	0	50	4	40	2.1
		1	1						
		2	0.78						
		6	0.37						
		10	0.25						
		50	0						
$u_{16} = 2.5$ eV		$u_{17} = 0.29$ eV		$u_{18} = 7$ eV		$u_{19} = 10.5$ eV		$u_{1,10} = 13.8$ eV	

Table 3.3: Tabulated data on the cross-sections for discharge pumping - continued 2

u_i	Q_{21}	u_i	Q_{22}	u_i	Q_{23}	u_i	Q_{24}	u_i	Q_{25}
0.29	0	1.83	0	1.9	0	2.05	0	2.1	0
0.5	0.0052	1.9	0.208	2	0.416	2.1	0.416	2.15	0.208
0.8	0.0083	2	1.46	2.1	1.33	2.2	1.16	2.2	0.541
1	0.0104	2.05	2.29	2.2	1.87	2.26	1.58	2.3	0.915
1.2	0.0166	2.1	1.66	2.3	1.25	2.55	0	2.46	1.12
1.3	0.0728	2.2	0.79	2.36	0.208	2.75	0.832	2.5	1.12
1.4	0.135	2.35	0.208	2.42	0	2.77	0	2.6	0.208
1.6	0.25	2.45	1.98	2.5	0.499	3	0.208	2.62	0
1.8	0.52	2.5	1.78	2.61	0.915	3.05	0.208	2.68	0
1.9	0.832	2.62	0.208	2.7	0.624	3.25	0	2.8	0.416
2	3.02	2.75	1.04	2.75	0.208			2.9	0.75
2.05	3.12	2.95	1.66	2.8	0			3	0
2.1	2.08	3.05	0.624	2.92	0.416			3.2	0.25
2.15	1.25	3.2	0.208	3	0.208			3.3	0.125
2.2	0.832	3.4	0.208	3.25	0.208			3.35	0
2.3	2.9	4	0	3.31	0				
2.45	1.04								
2.53	1.25								
2.6	1.75								
2.62	2.08								
2.68	1.73								
2.73	0.416								
2.85	0.32								
2.92	0.416								
3.12	0.728								
3.3	0.52								
4	0								
$u_{21} = 0.29$ eV		$u_{22} = 0.58$ eV		$u_{23} = 0.87$ eV		$u_{24} = 1.16$ eV		$u_{25} = 1.45$ eV	

u_i	Q_{26}	u_i	Q_{27}	u_i	Q_{28}	u_i	Q_{29}	u_i	$Q_{2,10}$
2.3	0	2.4	0	2.6	0	5	0	6.8	0
2.4	0.75	2.5	0.208	2.7	0.208	5.9	0.41	7.1	0.57
2.5	1.04	2.75	0.75	2.9	0.29	6.1	0.41	8.1	0.57
2.55	1.12	3	0	3	0.208	7	0.07	8.6	0.25
2.6	1.04	3.2	0.166	3.1	0	9	0	9.5	0.12
2.65	0.624	3.3	0.146	3.2	0			20.7	0
2.7	0.416	3.4	0	3.3	1.04				
2.8	0.208			3.4	0				
2.9	0.125								
3	2.5								
3.1	0.166								
3.2	0								
$u_{26} = 1.74$ eV		$u_{27} = 2.03$ eV		$u_{28} = 2.32$ eV		$u_{29} = 5$ eV		$u_{2,10} = 6.8$ eV	

u_i	$Q_{2,11}$	u_i	$Q_{2,12}$	u_i	$Q_{2,13}$	u_i	$Q_{2,14}$	u_i	$Q_{2,15}$
8.4	0	11.25	0	12.5	0	14	0	15.6	0
8.7	0.42	13.8	0.41	13	0.4	14.3	1.7	18	0.1
9.1	0.42	14	1	13.6	0.4	14.8	1.7	20	0.21
10	0.3	14.7	1	14	0.16	15.6	0.2	50	2.52
20.7	0	15	0.25	20.7	0	20.6	0.2	100	2.52
		65	0			25.4	2.8		
						100	2.8		
$u_{2,11} = 8.4$ eV		$u_{2,12} = 11.25$ eV		$u_{2,13} = 12.5$ eV		$u_{2,14} = 14$ eV		$u_{2,15} = 15.6$ eV	

Q_{m3} - Transport cross-section of He [6];
Q - Cross-section of resonant excitation of N_2 rotation [7, 8];
Q_{11} - Cross-section of the process $(000) \rightarrow (01^10)$ [6];
Q_{12} - Cross-section of the process $(000) \rightarrow (100 + 020)$ [6];
$Q_{13}...Q_{16}$ - Cross-sections of resonant processes around 3.8 eV [6];
Q_{17} - Cross-section of the process $(000) \rightarrow (001)$ [6];
$Q_{18}...Q_{1,10}$ - Cross-sections of electronic excitation and ionization of CO_2 [4];
$Q_{21}...Q_{28}$ - Cross-sections of the process $N_2(v = 0) \rightarrow N_2(v = 1...8)$ [9–11];
$Q_{29}...Q_{2,15}$ - Cross-sections of electronic excitation and ionization of N_2 [11].

Equation 3.1 is solved numerically using the tridiagonal matrix algorithm. Rate constant $omega_{jk}$ and electron drift speeds v_d are defined as:

$$\omega_{jk}\left[\frac{\mathrm{cm}^3}{\mathrm{s}}\right] = 5.93 \times 10^{-9} \int_0^\infty u Q_{jk}(u) f(u) du \tag{3.2}$$

$$v_d\left[\frac{\mathrm{cm}}{\mathrm{s}}\right] = -5.93 \times 10^7 \left(\frac{1}{3}\frac{E}{N}\right) \frac{df}{du} \int_0^\infty u \left(\sum_j y_j Q_{mj}(u)\right)^{-1} du \tag{3.3}$$

Fraction of electron energy transmitted via inelastic processes is defined as:

$$z_{jk} = 10^6 \frac{y_j u_{jk} \omega_{jk}}{\left(\frac{E}{N}\right) v_d} \tag{3.4}$$

Fraction of electron energy transmitted to translations and rotations are:

$$z_t = 5.93 \times 10^7 \frac{\int_0^\infty u^2 \left(\sum_j \frac{y_j}{M_j} Q_{mj}(u)\right) f(u) du}{\left(\frac{E}{N}\right) v_d} \tag{3.5}$$

$$z_r = 5.93 \times 10^7 \frac{\sum_{j=1,2} y_j C_j \int_0^\infty u f(u) du + 6 y_2 B \int_0^\infty u Q(u) f(u) du}{\left(\frac{E}{N}\right) v_d} \tag{3.6}$$

Then, for 4-temperature model we get:
$q_2 = \sum_{k=1}^{6} z_{1k}$ - fraction of energy transferred to CO_2 symmetric stretch (ν_1) and bending (ν_2) modes;
$q_3 = z_{17}$ - fraction of energy transferred to CO_2 asymmetric stretch mode (ν_3);
$q_4 = \sum_{k=1}^{8} z_{2k}$ - fraction of energy transferred to N_2 vibrations;
$q_T = z_t + z_r$ - fraction of energy transferred to translation and rotation;
$q_{ei} = \sum_{k=9}^{15} z_{2k} + \sum_{k=8}^{10} z_{1k}$ - fraction of energy spent on electronic levels excitation and ionization.

3.1.2 Pumping and vibrational relaxation dynamics

3-temperature model is used for describing vibrational dynamics of the laser system
T_2 – vibrational temperature of ν_1 and ν_2 vibrations ofCO_2;
T_3 – vibrational temperature of the ν_3 vibration of CO_2;
T_4 – vibrational temperature of N_2.
Vibrational temperatures are related to average number of quanta e_x in the corresponding vibrations as:

$$
\begin{aligned}
e_2 &= \frac{2}{\exp(960/T_2)-1} \\
e_3 &= \frac{1}{\exp(3380/T_3)-1} \\
e_4 &= \frac{1}{\exp(3350/T_4)-1}
\end{aligned}
\tag{3.7}
$$

("2" in the first equation is due to 2-fold degeneracy of the bend vibration levels).

Pumping/relaxation dynamics is described by the following equations [1]

$$
\begin{aligned}
\frac{de_4}{dt} &= p_{e4} - r_a(e_4 - e_3) \\
\frac{de_3}{dt} &= p_{e3} + r_c(e_4 - e_3) - r_3 f_3 \\
\frac{de_2}{dt} &= f_2\left(p_{e2} + 3r_3 f_3 - r_2(e_2 - e_{2T})\right)
\end{aligned}
\tag{3.8}
$$

where

$$
\begin{aligned}
&p_{e4} = 0.8\times10^{-3}\frac{q_4}{ny_2}W(t); \quad p_{e3} = 0.8\times10^{-3}\frac{q_3}{ny_1}W(t); \quad p_{e2} = 2.8\times10^{-3}\frac{q_2}{ny_1}W(t); \\
&f_2 = \frac{2(1+e_2)^2}{2+6e_2+3{e_2}^2}; \quad f_3 = e_3(1+e_2/2)^3 - (1+e_3)(e_2/2)^3\exp(-500/T); \\
&r_a = kny_1; \quad r_c = kny_2; \quad r_2 = k_2 n; \quad r_3 = k_3 n; \\
&k_2 = \sum_{i=1}^{3} y_i k_{2i}; \quad k_3 = \sum_{i=1}^{3} y_i k_{3i}; \\
&n = 273\frac{p[\mathrm{bar}]}{T_0[\mathrm{K}]},
\end{aligned}
$$

where $W(t)$ is measured in kW/cm^3 , p_e - in μs, and constants k are calculated using the following expressions [12, 13]:

$$
\begin{aligned}
k &= 240/T^{1/2}; \\
k_{31} &= A(t)\exp(4.138 + 7.945x - 631.24x^2 + 2239x^3); \\
k_{32} &= A(t)\exp(-1.863 + 213.3x - 2796.2x^2 + 9001.9x^3); \\
k_{33} &= A(t)\exp(-3.276 + 291.4x - 3831.8x^2 + 12688x^3); \\
k_{21} &= 1.16\times10^3\exp(-59.3x); \\
k_{22} &= 8.55\times10^2\exp(-69x); \\
k_{22} &= 1.3\times10^3\exp(-40.6x),
\end{aligned}
$$

where $x = T^{-1/3}$, $A(t) = (T/273)(1+e_{2T}/2)^{-3}$, and temperature is expressed in K.

Finally, the gas temperature dynamics is described by the Equation 3.9

$$
\frac{dT}{dt} = \frac{y_1}{C_V}(500r_3 f_3 + 960r_2(e_2 - e_{2T})) + 2.7\frac{W(t)q_T}{nC_V},
\tag{3.9}
$$

where $C_V = 2.5(y_1 + y_2) + 1.5y_3$.

3.2 Amplification

Amplification is simulated using the equations from Volkin's paper [14]

$$\begin{aligned}
&\frac{\partial \varepsilon}{\partial z} = -\sum_J \rho_J, \\
&\frac{\partial \rho_J}{\partial t} + \left(i(\omega_c - \omega_{0J}) + \frac{1}{T_2} \right) \rho_J = -\frac{\sigma_J n_J \varepsilon}{2T_2}, \\
&\frac{\partial n_J}{\partial t} + \frac{n_J - n_J^0}{\tau_R} = 4(\rho_J \varepsilon^* + c.c.),
\end{aligned} \tag{3.10}$$

where $\varepsilon(z,t)$ is the complex field envelope, ω_c the carrier frequency, ω_{0J} the frequency in the line center and σ_J the stimulated emission (or absorption) cross-section in the line center:

$$\sigma_J[\mathrm{m}^2] = \frac{(\lambda_J[\mathrm{m}])^2 A_J[\mathrm{s}^{-1}]}{4} \times \frac{T_2[\mathrm{s}]}{\pi},$$

where the first term defines the integral cross-section σ_0 of the rotational line [15] and the second term is the maximum of the normalized Lorentzian profile of a line with linewidth $\Delta\omega_{FWHM} = 2\pi\Delta\nu = 2/T_2$,

$$n_J^0 = z(J)(N^U - N^L),$$

where $z(J)$ is the Boltzmann distribution:

$$z(J) = 2\frac{hB}{kT}(2J+1)\exp\left(-\frac{hB}{kT}J(J+1)\right) \qquad 626, 636, 828, 838$$

$$z(J) = \frac{hB}{kT}(2J+1)\exp\left(-\frac{hB}{kT}J(J+1)\right) \qquad 628, 638$$

$h = 6.62606957 \times 10^{-34}$ J·s
$k = 1.3806488 \times 10^{-23}$ J/K
B: [s^{-1}]
T: [K]
Field amplitude is related to the intensity as follows:

$$I[\mathrm{W/m}^2] = 2h[\mathrm{J{\cdot}s}]\nu_c[\mathrm{s}^{-1}]\varepsilon^2 \tag{3.11}$$

Additional equations:

$$\begin{aligned}
&\frac{d}{dt}N^U = 2\sum_J (\rho_J \varepsilon_J^* + c.c.), \\
&\frac{d}{dt}N^{L10} = -2\sum_{J10} (\rho_J \varepsilon_J^* + c.c.), \\
&\frac{d}{dt}N^{L9} = -2\sum_{J9} (\rho_J \varepsilon_J^* + c.c.)
\end{aligned} \tag{3.12}$$

Relaxation times are defined from the following equations:

$$T_2[\mathrm{s}] = \frac{10^{-6}}{\pi \times 7.61 \times 750 \times (P_{CO2} + 0.733P_{N2} + 0.64P_{He})} \tag{3.13}$$

$$\tau_R[\text{s}] = \frac{10^{-7}}{750 \times (P_{CO2} + 1.2P_{N2} + 0.6P_{He})} \tag{3.14}$$

P is measured in Bar.

$$\Delta\nu_{FWHM} = \frac{1}{\pi T_2}$$

Useful relations for Lorentzian distribution:

$$\Delta\nu_{HWHM} = \frac{1}{2\pi T_2}; \quad \Delta\omega_{HWHM} = \frac{1}{T_2}$$

3.3 Molecular constants

bla-bla

3.4 Propagation

Beam propagation between layout elements is calculated using Huygens-Fresnel integration at each time-step of the pulse time-frame. In the general case, the field in a given position (x', y') of the output plane is calculated by integrating contributions from each point (x, y) of the input plane taken into account the phase delay.

$$E(x', y') = \int_x \int_y E(x, y) \frac{e^{ikR}}{i\lambda R} dxdy,$$

where k is the wave number, λ the wavelength, and R is the distance between points (x, y) in and (x', y') in the output plane: $R = \sqrt{(x - x')^2 + (y - y')^2 + \Delta z^2}$. Δz is the distance between the centers of the input and the output planes.

In the case of radially symmetric beam used in our model, calculations can be considerably accelerated by taken into account that the field is the same in all points at equal distance from the beam axis. In this case integration can be done by summing the contributions of concentric rings in the input plane as shown in the Fig. 3.1.

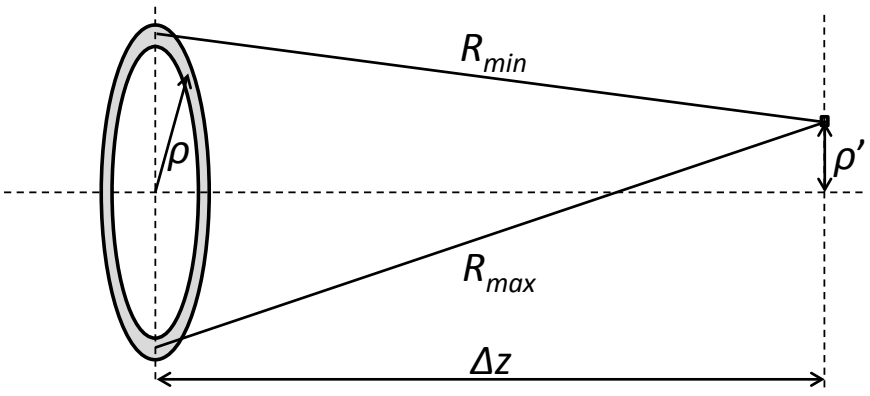

Figure 3.1: Huygens-Fresnel integration in the axial-symmetric system: Contribution of a field from a concentric ring in the input plane to a field in a point in the output plane.

The field in a given point with radial coordinate ρ' in the output plane is then calculated as

Table 3.4: Einstein coefficients A of laser transitions of *'626'* CO_2, s^{-1}

	Regular				Sequence				Hot-e				Hot-f			
J	10P	10R	9P	9R	10P	10R	9P	9R	10P	10R	9P	9R	10P	10R	9P	9R
0	-	0.134	-	0.149	-	-	-	-	-	-	-	-	-	-	-	-
1	-	-	-	-	0.824	0.331	0.812	0.326	-	0.108	-	0.131	-	-	-	-
2	0.267	0.172	0.296	0.192	-	-	-	-	-	-	-	-	0.179	0.137	0.216	0.167
3	-	-	-	-	0.493	0.369	0.486	0.364	0.191	0.150	0.230	0.182	-	-	-	-
4	0.229	0.183	0.252	0.205	-	-	-	-	-	-	-	-	0.191	0.158	0.231	0.191
5	-	-	-	-	0.456	0.383	0.449	0.379	0.190	0.162	0.229	0.197	-	-	-	-
6	0.218	0.188	0.240	0.211	-	-	-	-	-	-	-	-	0.189	0.166	0.228	0.201
7	-	-	-	-	0.440	0.392	0.434	0.388	0.187	0.168	0.226	0.204	-	-	-	-
8	0.212	0.191	0.234	0.216	-	-	-	-	-	-	-	-	0.186	0.170	0.224	0.207
9	-	-	-	-	0.432	0.396	0.425	0.394	0.185	0.171	0.223	0.209	-	-	-	-
10	0.209	0.193	0.230	0.219	-	-	-	-	-	-	-	-	0.184	0.173	0.222	0.210
11	-	-	-	-	0.425	0.400	0.420	0.399	0.183	0.174	0.221	0.212	-	-	-	-
12	0.206	0.194	0.227	0.221	-	-	-	-	-	-	-	-	0.183	0.175	0.219	0.213
13	-	-	-	-	0.421	0.402	0.416	0.403	0.182	0.175	0.219	0.214	-	-	-	-
14	0.204	0.195	0.225	0.224	-	-	-	-	-	-	-	-	0.181	0.176	0.218	0.215
15	-	-	-	-	0.417	0.404	0.413	0.406	0.181	0.177	0.217	0.216	-	-	-	-
16	0.203	0.196	0.223	0.226	-	-	-	-	-	-	-	-	0.180	0.177	0.216	0.217
17	-	-	-	-	0.413	0.405	0.411	0.409	0.179	0.178	0.215	0.218	-	-	-	-
18	0.201	0.197	0.221	0.228	-	-	-	-	-	-	-	-	0.179	0.178	0.214	0.218
19	-	-	-	-	0.410	0.406	0.409	0.412	0.178	0.179	0.213	0.219	-	-	-	-
20	0.200	0.197	0.220	0.230	-	-	-	-	-	-	-	-	0.178	0.179	0.213	0.220
21	-	-	-	-	0.407	0.407	0.408	0.415	0.177	0.180	0.212	0.220	-	-	-	-
22	0.198	0.197	0.219	0.231	-	-	-	-	-	-	-	-	0.177	0.180	0.211	0.221
23	-	-	-	-	0.404	0.407	0.406	0.417	0.176	0.180	0.211	0.222	-	-	-	-
24	0.197	0.197	0.218	0.233	-	-	-	-	-	-	-	-	0.176	0.181	0.210	0.222
25	-	-	-	-	0.400	0.407	0.405	0.421	0.175	0.181	0.209	0.223	-	-	-	-
26	0.196	0.197	0.217	0.235	-	-	-	-	-	-	-	-	0.175	0.181	0.209	0.223
27	-	-	-	-	0.397	0.407	0.404	0.423	0.174	0.182	0.208	0.224	-	-	-	-
28	0.195	0.197	0.216	0.237	-	-	-	-	-	-	-	-	0.174	0.182	0.207	0.224
29	-	-	-	-	0.395	0.406	0.403	0.425	0.174	0.182	0.207	0.225	-	-	-	-
30	0.193	0.197	0.215	0.238	-	-	-	-	-	-	-	-	0.173	0.182	0.206	0.225
31	-	-	-	-	0.392	0.406	0.402	0.428	0.173	0.183	0.205	0.225	-	-	-	-
32	0.192	0.196	0.215	0.240	-	-	-	-	-	-	-	-	0.172	0.183	0.205	0.226
33	-	-	-	-	0.388	0.406	0.402	0.431	0.172	0.183	0.204	0.226	-	-	-	-
34	0.191	0.196	0.214	0.242	-	-	-	-	-	-	-	-	0.171	0.183	0.203	0.226
35	-	-	-	-	0.385	0.405	0.401	0.434	0.171	0.183	0.203	0.227	-	-	-	-
36	0.189	0.196	0.213	0.244	-	-	-	-	-	-	-	-	0.170	0.183	0.202	0.227
37	-	-	-	-	0.383	0.403	0.401	0.437	0.170	0.184	0.202	0.228	-	-	-	-
38	0.188	0.195	0.213	0.246	-	-	-	-	-	-	-	-	0.169	0.184	0.201	0.228
39	-	-	-	-	0.380	0.402	0.400	0.439	0.169	0.184	0.201	0.229	-	-	-	-
40	0.187	0.194	0.212	0.248	-	-	-	-	-	-	-	-	0.168	0.184	0.200	0.229
41	-	-	-	-	0.376	0.401	0.399	0.442	0.168	0.185	0.199	0.229	-	-	-	-
42	0.185	0.194	0.212	0.249	-	-	-	-	-	-	-	-	0.168	0.184	0.198	0.229
43	-	-	-	-	0.373	0.400	0.400	0.446	0.167	0.185	0.198	0.230	-	-	-	-
44	0.184	0.193	0.211	0.251	-	-	-	-	-	-	-	-	0.167	0.185	0.197	0.230
45	-	-	-	-	0.369	0.398	0.400	0.448	0.167	0.185	0.197	0.231	-	-	-	-
46	0.182	0.192	0.211	0.253	-	-	-	-	-	-	-	-	0.166	0.185	0.196	0.230
47	-	-	-	-	0.366	0.397	0.400	0.451	0.166	0.185	0.196	0.231	-	-	-	-
48	0.181	0.191	0.210	0.255	-	-	-	-	-	-	-	-	0.165	0.185	0.195	0.231
49	-	-	-	-	0.362	0.394	0.400	0.455	0.165	0.186	0.194	0.232	-	-	-	-
50	0.179	0.191	0.210	0.257	-	-	-	-	-	-	-	-	0.164	0.185	0.193	0.232
51	-	-	-	-	0.359	0.393	0.399	0.458	0.164	0.186	0.193	0.232	-	-	-	-
52	0.178	0.190	0.209	0.259	-	-	-	-	-	-	-	-	0.163	0.185	0.192	0.232
53	-	-	-	-	0.354	0.391	0.401	0.462	0.163	0.186	0.192	0.233	-	-	-	-
54	0.176	0.189	0.209	0.262	-	-	-	-	-	-	-	-	0.162	0.185	0.191	0.233
55	-	-	-	-	0.351	0.388	0.401	0.464	0.162	0.186	0.191	0.234	-	-	-	-
56	0.174	0.187	0.209	0.264	-	-	-	-	-	-	-	-	0.161	0.186	0.189	0.233
57	-	-	-	-	0.347	0.385	0.400	0.467	0.161	0.186	0.189	0.234	-	-	-	-
58	0.173	0.186	0.209	0.266	-	-	-	-	-	-	-	-	0.160	0.186	0.188	0.234
59	-	-	-	-	0.344	-	0.401	0.471	0.160	0.186	0.188	0.234	-	-	-	-
60	0.171	-	0.208	-	-	-	-	-	-	-	-	-	0.159	-	0.187	-

Table 3.5: Einstein coefficients A of laser transitions of *'628'* CO_2, s^{-1}

	Regular				Sequence				Hot-e				Hot-f			
J	10P	10R	9P	9R	10P	10R	9P	9R	10P	10R	9P	9R	10P	10R	9P	9R
0	-	0.101	-	0.190												
1	0.303	0.122	0.569	0.229												
2	0.202	0.131	0.379	0.246		- no data -				- no data -				- no data -		
3	0.181	0.136	0.340	0.256												
4	0.172	0.140	0.323	0.262												
5	0.167	0.142	0.314	0.266												
6	0.163	0.144	0.307	0.270												
7	0.161	0.145	0.303	0.273												
8	0.159	0.147	0.299	0.275												
9	0.157	0.148	0.296	0.277												
10	0.156	0.149	0.294	0.279												
11	0.155	0.150	0.292	0.280												
12	0.154	0.150	0.290	0.282												
13	0.153	0.151	0.288	0.283												
14	0.152	0.152	0.287	0.284												
15	0.151	0.152	0.285	0.285												
16	0.151	0.153	0.284	0.286												
17	0.150	0.153	0.283	0.287												
18	0.149	0.154	0.282	0.288												
19	0.149	0.154	0.281	0.289												
20	0.148	0.155	0.280	0.290												
21	0.148	0.155	0.279	0.290												
22	0.147	0.156	0.278	0.291												
23	0.146	0.156	0.277	0.292												
24	0.146	0.157	0.276	0.293												
25	0.145	0.157	0.275	0.293												
26	0.145	0.157	0.274	0.294												
27	0.144	0.158	0.273	0.295												
28	0.144	0.158	0.272	0.295												
29	0.143	0.158	0.271	0.296												
30	0.143	0.159	0.271	0.297												
31	0.142	0.159	0.270	0.297												
32	0.142	0.159	0.269	0.298												
33	0.141	0.160	0.268	0.298												
34	0.141	0.160	0.267	0.299												
35	0.140	0.160	0.266	0.300												
36	0.140	0.161	0.266	0.300												
37	0.139	0.161	0.265	0.301												
38	0.139	0.161	0.264	0.301												
39	0.138	0.161	0.263	0.302												
40	0.138	0.162	0.262	0.302												
41	0.137	0.162	0.262	0.303												
42	0.137	0.162	0.261	0.303												
43	0.136	0.163	0.260	0.304												
44	0.136	0.163	0.259	0.304												
45	0.135	0.163	0.258	0.304												
46	0.135	0.163	0.258	0.305												
47	0.134	0.164	0.257	0.305												
48	0.134	0.164	0.256	0.306												
49	0.133	0.164	0.255	0.306												
50	0.133	0.164	0.254	0.307												
51	0.133	0.165	0.254	0.307												
52	0.132	0.165	0.253	0.308												
53	0.132	0.165	0.252	0.308												
54	0.132	0.165	0.251	0.309												
55	0.132	0.165	0.250	0.309												
56	0.132	0.165	0.250	0.309												
57	0.132	0.165	0.249	0.310												
58	0.132	0.165	0.248	0.310												
59	0.132	0.165	0.248	0.310												
60	0.132	-	0.248	-												

Table 3.6: Einstein coefficients A of laser transitions of *'828'* CO_2, s^{-1}

	Regular				Sequence				Hot-e				Hot-f			
J	10P	10R	9P	9R	10P	10R	9P	9R	10P	10R	9P	9R	10P	10R	9P	9R
0	-	0.038	-	0.121												
1	-	-	-	-												
2	0.075	0.048	0.240	0.156		- no data -				- no data -				- no data -		
3	-	-	-	-												
4	0.064	0.051	0.204	0.166												
5	-	-	-	-												
6	0.061	0.053	0.195	0.171												
7	-	-	-	-												
8	0.059	0.054	0.190	0.175												
9	-	-	-	-												
10	0.059	0.054	0.187	0.178												
11	-	-	-	-												
12	0.058	0.054	0.184	0.179												
13	-	-	-	-												
14	0.057	0.055	0.183	0.182												
15	-	-	-	-												
16	0.057	0.055	0.181	0.183												
17	-	-	-	-												
18	0.056	0.055	0.179	0.185												
19	-	-	-	-												
20	0.056	0.055	0.178	0.187												
21	-	-	-	-												
22	0.056	0.055	0.178	0.187												
23	-	-	-	-												
24	0.055	0.055	0.177	0.189												
25	-	-	-	-												
26	0.055	0.055	0.176	0.191												
27	-	-	-	-												
28	0.055	0.055	0.175	0.192												
29	-	-	-	-												
30	0.054	0.055	0.174	0.193												
31	-	-	-	-												
32	0.054	0.055	0.174	0.195												
33	-	-	-	-												
34	0.054	0.055	0.174	0.196												
35	-	-	-	-												
36	0.053	0.055	0.173	0.198												
37	-	-	-	-												
38	0.053	0.055	0.173	0.200												
39	-	-	-	-												
40	0.052	0.054	0.172	0.201												
41	-	-	-	-												
42	0.052	0.054	0.172	0.202												
43	-	-	-	-												
44	0.052	0.054	0.171	0.204												
45	-	-	-	-												
46	0.051	0.054	0.171	0.205												
47	-	-	-	-												
48	0.051	0.054	0.170	0.207												
49	-	-	-	-												
50	0.050	0.054	0.170	0.208												
51	-	-	-	-												
52	0.050	0.053	0.170	0.210												
53	-	-	-	-												
54	0.049	0.053	0.170	0.213												
55	-	-	-	-												
56	0.049	0.052	0.170	0.214												
57	-	-	-	-												
58	0.049	0.052	0.170	0.216												
59	-	-	-	-												
60	0.048	-	0.169	-												

Table 3.7: Einstein coefficients A of laser transitions of *'636'* CO_2, s^{-1}

	Regular				Sequence				Hot-e				Hot-f			
J	10P	10R	9P	9R	10P	10R	9P	9R	10P	10R	9P	9R	10P	10R	9P	9R
0	-	0.147	-	0.077												
1	-	-	-	-												
2	0.293	0.189	0.153	0.099		- no data -				- no data -				- no data -		
3	-	-	-	-												
4	0.251	0.201	0.131	0.106												
5	-	-	-	-												
6	0.239	0.207	0.124	0.109												
7	-	-	-	-												
8	0.233	0.210	0.121	0.111												
9	-	-	-	-												
10	0.229	0.212	0.119	0.113												
11	-	-	-	-												
12	0.226	0.214	0.118	0.114												
13	-	-	-	-												
14	0.224	0.215	0.117	0.115												
15	-	-	-	-												
16	0.222	0.216	0.116	0.116												
17	-	-	-	-												
18	0.220	0.216	0.115	0.117												
19	-	-	-	-												
20	0.219	0.217	0.114	0.118												
21	-	-	-	-												
22	0.217	0.217	0.114	0.119												
23	-	-	-	-												
24	0.216	0.217	0.113	0.120												
25	-	-	-	-												
26	0.215	0.217	0.113	0.121												
27	-	-	-	-												
28	0.213	0.217	0.112	0.122												
29	-	-	-	-												
30	0.212	0.217	0.112	0.122												
31	-	-	-	-												
32	0.210	0.217	0.112	0.123												
33	-	-	-	-												
34	0.209	0.216	0.111	0.124												
35	-	-	-	-												
36	0.207	0.216	0.111	0.125												
37	-	-	-	-												
38	0.206	0.215	0.111	0.126												
39	-	-	-	-												
40	0.204	0.215	0.111	0.127												
41	-	-	-	-												
42	0.203	0.214	0.110	0.128												
43	-	-	-	-												
44	0.201	0.214	0.110	0.129												
45	-	-	-	-												
46	0.199	0.213	0.110	0.130												
47	-	-	-	-												
48	0.198	0.212	0.110	0.131												
49	-	-	-	-												
50	0.196	0.211	0.110	0.132												
51	-	-	-	-												
52	0.194	0.210	0.110	0.133												
53	-	-	-	-												
54	0.192	0.209	0.109	0.133												
55	-	-	-	-												
56	0.191	0.208	0.109	0.133												
57	-	-	-	-												
58	0.191	0.208	0.109	0.133												
59	-	-	-	-												
60	0.191	-	0.109	-												

Table 3.8: Einstein coefficients A of laser transitions of *'638'* CO_2, s^{-1}

	Regular				Sequence				Hot-e				Hot-f			
J	10P	10R	9P	9R	10P	10R	9P	9R	10P	10R	9P	9R	10P	10R	9P	9R
0	-	0.382	-	0.330												
1	0.126	0.256	0.109	0.221												
2	0.151	0.231	0.131	0.199		- no data -				- no data -				- no data -		
3	0.161	0.221	0.140	0.190												
4	0.167	0.216	0.144	0.186												
5	0.170	0.213	0.147	0.183												
6	0.171	0.211	0.149	0.181												
7	0.173	0.209	0.150	0.180												
8	0.173	0.209	0.151	0.179												
9	0.174	0.208	0.152	0.179												
10	0.174	0.208	0.152	0.178												
11	0.174	0.208	0.152	0.178												
12	0.174	0.208	0.153	0.178												
13	0.173	0.208	0.153	0.179												
14	0.173	0.208	0.153	0.179												
15	0.173	0.208	0.153	0.179												
16	0.172	0.208	0.153	0.179												
17	0.171	0.209	0.153	0.180												
18	0.171	0.209	0.152	0.180												
19	0.170	0.209	0.152	0.181												
20	0.169	0.210	0.152	0.181												
21	0.169	0.210	0.152	0.182												
22	0.168	0.210	0.152	0.182												
23	0.167	0.211	0.152	0.182												
24	0.167	0.211	0.152	0.183												
25	0.166	0.211	0.152	0.184												
26	0.165	0.212	0.151	0.184												
27	0.164	0.212	0.151	0.185												
28	0.163	0.212	0.151	0.186												
29	0.162	0.213	0.150	0.186												
30	0.162	0.213	0.150	0.187												
31	0.161	0.213	0.150	0.188												
32	0.160	0.214	0.150	0.188												
33	0.159	0.214	0.150	0.189												
34	0.158	0.214	0.150	0.190												
35	0.157	0.215	0.150	0.191												
36	0.156	0.215	0.149	0.192												
37	0.155	0.215	0.149	0.192												
38	0.154	0.216	0.149	0.193												
39	0.153	0.216	0.149	0.194												
40	0.152	0.216	0.149	0.195												
41	0.151	0.217	0.148	0.195												
42	0.151	0.217	0.148	0.196												
43	0.149	0.217	0.148	0.197												
44	0.148	0.217	0.148	0.198												
45	0.148	0.217	0.148	0.199												
46	0.146	0.218	0.147	0.200												
47	0.145	0.218	0.147	0.201												
48	0.144	0.218	0.147	0.202												
49	0.143	0.218	0.147	0.203												
50	0.142	0.218	0.147	0.204												
51	0.141	0.218	0.147	0.205												
52	0.140	0.219	0.147	0.206												
53	0.139	0.219	0.146	0.207												
54	0.138	0.219	0.146	0.208												
55	0.137	0.219	0.146	0.209												
56	0.136	0.219	0.146	0.210												
57	0.135	0.219	0.146	0.211												
58	0.134	0.219	0.146	0.212												
59	0.133	0.219	0.146	0.213												
60	0.132	-	0.145	-												

Table 3.9: Einstein coefficients A of laser transitions of *'838'* CO_2, s^{-1}

	Regular				Sequence				Hot-e				Hot-f			
J	10P	10R	9P	9R	10P	10R	9P	9R	10P	10R	9P	9R	10P	10R	9P	9R
0	-	0.053	-	0.070												
1	-	-	-	-												
2	0.105	0.068	0.138	0.090		- no data -				- no data -				- no data -		
3	-	-	-	-												
4	0.090	0.072	0.118	0.096												
5	-	-	-	-												
6	0.086	0.074	0.112	0.098												
7	-	-	-	-												
8	0.083	0.075	0.109	0.101												
9	-	-	-	-												
10	0.082	0.076	0.107	0.102												
11	-	-	-	-												
12	0.081	0.076	0.106	0.103												
13	-	-	-	-												
14	0.080	0.077	0.105	0.105												
15	-	-	-	-												
16	0.080	0.077	0.104	0.105												
17	-	-	-	-												
18	0.079	0.077	0.103	0.106												
19	-	-	-	-												
20	0.079	0.077	0.103	0.107												
21	-	-	-	-												
22	0.078	0.077	0.102	0.108												
23	-	-	-	-												
24	0.077	0.077	0.102	0.109												
25	-	-	-	-												
26	0.077	0.077	0.101	0.110												
27	-	-	-	-												
28	0.077	0.077	0.101	0.111												
29	-	-	-	-												
30	0.076	0.077	0.100	0.111												
31	-	-	-	-												
32	0.075	0.077	0.100	0.112												
33	-	-	-	-												
34	0.075	0.077	0.100	0.113												
35	-	-	-	-												
36	0.074	0.077	0.099	0.114												
37	-	-	-	-												
38	0.074	0.077	0.099	0.115												
39	-	-	-	-												
40	0.073	0.076	0.099	0.116												
41	-	-	-	-												
42	0.073	0.076	0.099	0.116												
43	-	-	-	-												
44	0.072	0.076	0.098	0.117												
45	-	-	-	-												
46	0.071	0.075	0.098	0.118												
47	-	-	-	-												
48	0.071	0.075	0.098	0.119												
49	-	-	-	-												
50	0.070	0.075	0.098	0.120												
51	-	-	-	-												
52	0.070	0.075	0.098	0.121												
53	-	-	-	-												
54	0.069	0.074	0.098	0.122												
55	-	-	-	-												
56	0.068	0.073	0.098	0.123												
57	-	-	-	-												
58	0.068	0.073	0.098	0.124												
59	-	-	-	-												
60	0.067	-	0.097	-												

$$E(\rho') = \int_\rho E(\rho) \frac{e^{-ikR}}{i\lambda R} J_0(k\Delta R/2) dS \tag{3.15}$$

where $dS = \pi(\rho + d\rho/2)^2 - \pi(\rho - d\rho/2)^2$ is the area of the ring, $R = (R_{max} + R_{min})/2$, $\Delta R = R_{max} - R_{min}$, $R_{max} = \sqrt{(\rho + \rho')^2 + \Delta z^2}$, $R_{min} = \sqrt{(\rho - \rho')^2 + \Delta z^2}$, and J_0 is the Bessel function.

3.5 Optical elements

Optical elements change the electric field as described by the following formulas. In these formulas $E(t, \rho)$ is the field in the input of the element and $E'(t, \rho)$ - after passing through the element.

Probe

(*Passive surface, may be used as limiting aperture*)

$$E'(t, \rho) = E(t, \rho),$$

Mask

(*Opaque circular screen*)

$$\begin{aligned} E'(t, \rho) &= 0, & \rho < R \\ E'(t, \rho) &= E(t, \rho), & \rho \geq R \end{aligned}$$

where R is the radius of the mask.

Absorber

(*Ideal ND filter*)

$$E'(t, \rho) = E(t, \rho)\sqrt{T},$$

where T is the transmittance.

Lens

(*Ideal lens without aberrations*)

$$E'(t, \rho) = E(t, \rho) \exp\left(\pi i \frac{\rho^2}{\lambda_c F}\right),$$

where F is the focal length of the lens and λ_c is the central wavelength.

Window

(*Flat transparent window with zero reflection- and absorption- losses*)

Linear dispersion

$$\begin{aligned} &\widehat{E}(\nu, \rho) = \mathcal{F}(E(t, \rho)), \\ &\widehat{E}'(\nu, \rho) = \widehat{E}(\nu, \rho) \exp\left(-2\pi i \nu \frac{\Theta}{c}\left(n_0(\nu) - n_0(\nu_c) - \nu_c \frac{dn_0}{d\nu}\right)\right), \\ &E'(t, \rho) = \mathcal{F}^{-1}(\widehat{E}'(\nu, \rho)), \end{aligned}$$

where $\widehat{E}(\nu,\rho)$ is the field in the frequency domain, $\mathcal{F}$ and $\mathcal{F}^{-1}$ the Fourier transform and inverse Fourier transform functions, ν the frequency, ν_c the central frequency, n_0 is the linear component of the index of refraction and Θ is the thickness of the window.

Nonlinear interaction

$$E'(t,\rho) = E(t,\rho)\exp\left(-2\pi i\nu_c\frac{\Theta}{c}n_2 I(t,\rho)\right),$$

where n_2 is the nonlinear refractive index and $I(t,\rho)$ is the field intensity.

Stretcher

(*Stretcher or compressor*)

$$\begin{aligned}
&\widehat{E}(\nu,\rho) = \mathcal{F}(E(t,\rho)),\\
&\widehat{E}'(\nu,\rho) = \widehat{E}(\nu,\rho)\exp\left(-\pi i(\nu-\nu_c)^2 S\right),\\
&E'(t,\rho) = \mathcal{F}^{-1}(\widehat{E}(\nu,\rho)),
\end{aligned}$$

where S is the stretching factor (in s/Hz, positive for red chirp).

3.6 Properties of optical materials

The following expressions and values for linear- (n_0) and nonlinear- (n_2) refractive indexes are used in the program (wavelength λ in the dispersion formulas must be expressed in μm):

CdTe

$n_0 = \sqrt{1 + \frac{6.1977889\lambda^2}{\lambda^2-0.1005326} + \frac{3.2243821\lambda^2}{\lambda^2-5279.518}}$ [16]
$n_2 = -2.95\times10^{-13}$ cm^2/W at 1.06 μm [17]

GaAs

$n_0 = \sqrt{5.372514 + \frac{5.466742\lambda^2}{\lambda^2-0.4431307^2} + \frac{0.02429960\lambda^2}{\lambda^2-0.8746453^2} + \frac{1.957522\lambda^2}{\lambda^2-36.9166^2}}$ [18]
$n_2 = -3.26\times10^{-13}$ m^2/W at 1.06 μm [17]

Ge

$n_0 = \sqrt{9.28156 + \frac{6.72880\lambda^2}{\lambda^2-0.44105} + \frac{0.21307\lambda^2}{\lambda^2-3870.1}}$ [19]
$n_2 = 2.83\times10^{-13}$ cm^2/W at 10.6 μm [17]

KCl

$n_0 = \sqrt{1.26486 + \frac{0.30523\lambda^2}{\lambda^2-0.100^2} + \frac{0.41620\lambda^2}{\lambda^2-0.131^2} + \frac{0.18870\lambda^2}{\lambda^2-0.162^2} + \frac{2.6200\lambda^2}{\lambda^2-70.42^2}}$ [20]
$n_2 = 5.62\times10^{-16}$ cm^2/W at 1.06 μm [17]

NaCl

$n_0 = \sqrt{1.00055 + \frac{0.19800\lambda^2}{\lambda^2-0.050^2} + \frac{0.48398\lambda^2}{\lambda^2-0.100^2} + \frac{0.38696\lambda^2}{\lambda^2-0.128^2} + \frac{0.25998\lambda^2}{\lambda^2-0.158^2} + \frac{0.08796\lambda^2}{\lambda^2-40.50^2} + \frac{3.17064\lambda^2}{\lambda^2-60.98^2} + \frac{0.30038\lambda^2}{\lambda^2-120.34^2}}$ [20]
$n_2 = 4.38\times10^{-16}$ cm^2/W at 1.06 μm [17]

Si

$n_0 = 3.41983 + \frac{0.159906}{\lambda^2 - 0.028} - 0.123109 \left(\frac{1}{\lambda^2 - 0.028}\right)^2 + 1.26878 \times 10^{-6}\lambda^2 - 1.95104 \times 10^{-9}\lambda^4$ [21]
$n_2 = 1.0 \times 10^{-13}$ cm^2/W at 2.2 μm [22]

ZnSe

$n_0 = \sqrt{1 + \frac{4.45813734\lambda^2}{\lambda^2 - 0.200859853^2} + \frac{0.467216334\lambda^2}{\lambda^2 - 0.391371166^2} + \frac{2.89566290\lambda^2}{\lambda^2 - 47.1362108^2}}$ [23]
$n_2 = 2.87 \times 10^{-14}$ cm^2/W at 1.06 μm [17]

Bibliography

[1] N. V. Karlov and Y. B. Konev. High pressure pulsed CO_2 lasers. In A. M. Prokhorov, editor, *Handbook on lasers*. Sovetskoe Radio, Moscow, 1978 (in Russian).

[2] T. Holstein. Energy distribution of electrons in high frequency gas discharges. *Phys. Rev.*, 70:367–384, 1946.

[3] W. L. Nighan. Electron energy distributions and collision rates in electrically excited N_2, CO, and CO_2. *Phys. Rev. A*, 2:1989–2000, 1970.

[4] R. D. Hake and A. V. Phelps. Momentum-transfer and inelastic-collision cross sections for electrons in O_2, CO, and CO_2. *Phys. Rev.*, 158:70–84, 1967.

[5] L. S. Frost and A. V. Phelps. Rotational excitation and momentum transfer cross sections for electrons in H_2 and N_2 from transport coefficients. *Phys. Rev.*, 127:1621–1633, 1962.

[6] J. J. Lowke, A. V. Phelps, and B. W. Irwin. Predicted electron transport coefficients and operating characteristics of CO_2-N_2-He laser mixtures. *J. Appl. Phys.*, 44:4664–4671, 1973.

[7] Y. D. Oksyuk. Excitation of the rotational levels of diatomic molecules by electron impact in the adiabatic approximation. *Sov. J. Exp. Theor. Phys.*, 22:873, 1966.

[8] N. Chandra and P. G. Burke. Rotational excitation cross sections for e^--N_2 scattering. *J. Phys. B: At. Mol. Phys.*, 6:2355–2357, 1973.

[9] A. V. Phelps. Rotational and vibrational excitation of molecules by low-energy electrons. *Rev. Mod. Phys.*, 40:399–410, 1968.

[10] G. J. Schulz. Vibrational excitation of nitrogen by electron impact. *Phys. Rev.*, 125:229–232, 1962.

[11] A. G. Engelhardt, A. V. Phelps, and C. G. Risk. Excitation of the rotational levels of diatomic molecules by electron impact in the adiabatic approximation. *Phys. Rev.*, 135:A1566–A1574, 1964.

[12] A. S. Biryukov, V. K. Konyukhov, A. I. Lukovnikov, and R. I. Serikov. Relaxation of the vibrational energy of the (00^01) level of the CO_2 molecule. *Sov. J. Exp. Theor. Phys.*, 39:610, 1974.

[13] R. L. Taylor and S. Bitterman. Survey of vibrational relaxation data for processes important in the CO_2-N_2 laser system. *Rev. Mod. Phys.*, 41:26–47, 1969.

[14] H. C. Volkin. Calculation of short-pulse propagation in a large CO_2-laser amplifier. *J. Appl. Phys.*, 50:1179–1188, 1979.

[15] R. D. Hake and A. V. Phelps. Einstein coefficients, cross sections, f values, dipole moments, and all that. *arXiv:physics/0202029*, 2002.

[16] A. G. DeBell, E. L. Dereniak, J. Harvey, J. Palmer J. Nissley, A. Selvarajan, and W. L. Wolfe. Cryogenic refractive indices and temperature coefficients of cadmium telluride from 6 μm to 22 μm. *Appl. Opt.*, 18:3114–3115, 1979.

[17] M. Sheik-Bahae. Dispersion of bound electron nonlinear refraction in solids. *IEEE J. Quant. Electron.*, 27:1296–1309, 1991.

[18] T. Skauli, P. S. Kuo, K. L. Vodopyanov, T. J. Pinguet, O. Levi, L. A. Eyres, J. S. Harris, M. M. Fejer, L. Becouarn B. Gerard, and E. Lallier. Improved dispersion relations for gaas and applications to nonlinear optics. *J. Appl. Opt.*, 94:6447–6455, 2003.

[19] N. P. Barnes and M. S. Piltch. Temperature-dependent sellmeier coefficients and nonlinear optics average power limit for germanium. *J. Opt. Soc. Am.*, 69:178–180, 1979.

[20] H. H. Li. Refractive index of alkali halides and its wavelength and temperature derivatives. *J. Phys. Chem. Ref. Data*, 5:329–528, 1976.

[21] D. F. Edwards and E. Ochoa. Infrared refractive index of silicon. *Appl. Opt.*, 19:4130–4131, 1980.

[22] A. D. Bristow, N. Rotenberg, and H. M. van Driel. Two-photon absorption and kerr coefficients of silicon for 850–2200 nm. *Appl. Phys. Lett.*, 90:191104, 2007.

[23] B. Tatian. Fitting refractive-index data with the sellmeier dispersion formula. *Appl. Opt.*, 23:4477–4485, 1984.